REPORT DOCUMENTATION PAGE

OMB No. 0704-0188

1. AGENCY USE ONLY (Leave blank)	2. REPORT DATE	3. REPORT TYPE AND DATES COVERED
	6/29/95	Final Technical Report, 4/15/94-4/14/95

4. TITLE AND SUBTITLE

Local preconditioning of the Euler equations and its numerical applications

5. FUNDING NUMBERS

AFOSR Grant No.
F49620-92-J-0158DEF

6. AUTHOR(S)

Bram van Leer
and Philip L. Roe

7. PERFORMING ORGANIZATION NAME(S) AND ADDRESS(ES)

W.M. Keck Foundation Laboratory for Computational Fluid Dynamics
Department of Aerospace Engineering
The University of Michigan
Ann Arbor MI 48109-2118

8. PERFORMING ORGANIZATION REPORT NUMBER

AFOSR-TR-95

0655

9. SPONSORING/MONITORING AGENCY NAME(S) AND ADDRESS(ES)

AFOSR
Major Scott Schreck, Program Manager
Computational Mathematics
Directorate of Mathematical and Computer Sciences
Bolling AFB DC

11. SUPPLEMENTARY NOTES

12a. DISTRIBUTION/AVAILABILITY STATEMENT

[redacted] Unlimited

12b. DISTRIBUTION CODE

13. ABSTRACT (Maximum 200 words)

The stagnation-point instability has been remedied by two measures:

1. The sensitivity of the Van Leer preconditioner to the flow angle for low Mach number was reduced at the cost of raising the characteristic condition number from 1 to 2.
2. One matric element was bounded away from zero so as to prevent certain eigenvectors to become parallel in the limit of vanishing Mach number.

Navier-Stokes preconditioners were studied at low cell Reynolds number, as was preconditioning in the presence of a one-equation turbulence model.
The results over the entire 3-year contract period are reviewed.

14. SUBJECT TERMS

computational fluid dynamics
inviscid compressible flow
stiff systems of partial differential equations

15. NUMBER OF PAGES

5(not counting 2 re-

16. PRICE CODE

prints

17. SECURITY CLASSIFICATION OF REPORT	18. SECURITY CLASSIFICATION OF THIS PAGE	19. SECURITY CLASSIFICATION OF ABSTRACT	20. LIMITATION OF ABSTRACT
UNCLASSIFIED	UNCLASSIFIED	UNCLASSIFIED	

Local preconditioning of the Euler equations and its numerical applications

Final technical report to AFOSR

regarding AFOSR Grant No. F49620-92-J-0158-DEF

Bram van Leer and Philip L. Roe
W. M. Keck Laboratory for Computational Fluid Dynamics
Department of Aerospace Engineering
The University of Michigan

1 General information

This is the final technical report on research carried out under Air Force Grant No. F49620-92-J-0158-DEF, in the period April 15, 1992 - April 14, 1995. The project title was "Local preconditioning of the Euler equations and its numerical applications." It was awarded for research exploiting the recent discovery of local preconditioning matrices that minimize the spread among the wave speeds admitted by the Euler equations for any Mach number. Closely related to this research is the work carried out under Augmentation Grant No. F49620-93-1-0417; its project title is "Efficient explicit integration schemes for the hyperbolized Navier-Stokes equations." This project considers the application of local preconditioning to a stiff hyperbolic system describing viscous conducting flow with a finite relaxation time. Over the past year part of the effort in this subject was diverted to the main subject in order to help solve the problem of the stagnation-point instability (see below), which was halting progress in both principal and augmentation projects. Where relevant, research findings from the augmentation project are included below.

2 Research in the past year

Since the previous report research under the principal grant has focussed on the problem of instability in stagnation regions, experienced in the use of a variety of inviscid flow codes: conservative and nonconservative, cell-average and cell-vertex based.

In July-August '95 a concentrated effort (not funded by AFOSR) of some developers and users of local preconditioning at ICASE/NASA Langley Research Center led to a modification of the Van Leer preconditioning that makes this matrix insensitive to the flow direction near stagnation points, where the flow direction is ill-determined. The modified matrix immediately cured the stability and accuracy problems for the

cell-vertex, fluctuation-split, nonconservative code of Lisa Mesaros (doctoral candidate, U. of MI); the conservative version of her code was not helped very much by the modification. This suggested that there was yet another cause of the stagnation-point difficulties.

Subsequently, David Darmofal (NSF/AFOSR post-doc, U., of MI), in collaboration with Peter Schmid (U. of WA), studied the eigenvector structure of the matrices arising in the preconditioned Euler equations. He concluded that the main problem for vanishing flow speed or Mach number M is the large deviation from orthogonality of the eigenvectors: certain eigenvectors become parallel for $M \to 0$. When marching to a steady solution this causes a strong initial transient that may lead to instability.

Based on this analysis a modification was proposed for preconditioning matrices of the Van Leer-Turkel family; the modified matrices were successfully implemented in an unstructured conservative code. This marks the first time that the stability problem has been removed in the use of a conservative code. The modification consists of downward limiting of the Mach-number value used in the (1,1) matrix element ($\sim M^2$), e.g. by a minimum value that is a small fraction of the far-field Mach number. In previous "fixes" the Mach number was limited everywhere in the preconditioning matrix and its products with other matrices; apparently this does not affect the numerical fluxes in a desirable way.

We expect the new modified preconditioner to solve the stagnation problems of other conservative preconditioned codes; this is currently under investigation in other projects.

The application of the Van Leer preconditioning to the design of multi-stage marching scheme with optimal high-frequency damping, and the use of such schemes in a multi-grid relaxation framework, are the subject of a thesis by John Lynn, defended in our Department on May 17, 1995. He has shown that the double benefit of preconditioning, known from one-dimensional calculations by Tai (Ph.D., U. of MI, 1990), persists in two dimensions. The preconditioning already speeds up single-grid relaxation; the guaranteed high-frequency damping of the optimized multi-stage schemes provides an extra speed-up of a factor 2-3, and additional robustness.

The thesis includes tables of recommended multi-stage coefficients, and also discusses the extensions to Navier-Stokes operators and to unstructured grids. In the numerical examples Lynn avoided the stagnation-point instability by avoiding flow problems including stagnation points.

The above research has been reported at the 12th AIAA Conference on Computational Fluid Dynamics, June 19 - 22, San Diego, CA. Two conference papers were prepared under the principal AFOSR grant; these are listed below.

1. B. van Leer, L. Mesaros, C.-H. Tai and E. Turkel, "Local preconditioning in a stagnation point," AIAA Paper 95-1654CP, 1995.

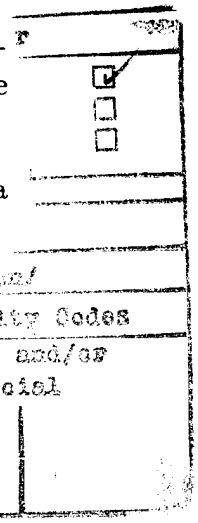

2. J. F. Lynn and B. van Leer, "A semi-coarsened multi-grid solver for the Euler and Navier-Stokes equations with local precnditioning," AIAA Paper 95-1667CP, 1995.

The remainder of the research was dedicated to further development of the preconditioning matrix for the Navier-Stokes equations so as to make it useful for very low cell Reynolds-numbers. Preconditioning in the presence of a one-equation turbulence model (Spalart-Allmaras) has also been investigated. Neither subject has been rounded off.

3 Review of results from entire contract period

During the contract period of three years major progress was made in the understanding, application and improvement of local preconditioning for the Euler and Navier-Stokes equations. One of the foremost results is the demonstration that the use of our Euler preconditioner in two space dimension yields a *double* benefit in a multi-grid strategy: a single-grid speed-up factor, owing to removal of system stiffness, and an independent multi-grid speed-up factor, owing to guaranteed high-frequency damping. These results are contained in the Ph.D. thesis of John Lynn, whose doctoral work was supported by the contract over the last 18 months. It is worth noticing that among researchers that use local preconditioning for the sake of multi-grid relaxation, almost all select point-Jacobi preconditioning, which only gives the *second* bewnefit.

Basic understanding of the potential possibilities present in the family of optimal Euler preconditioners was obtained. It turned out that, in spite of the overwhelming number of free parameters, much of the parameter space is irrelevant. The symmetric Van Leer-Lee-Roe 2 parameter preconditioning matrix, on which this contract was based, turns out to be the most desirable form under all circumstances. For very low Mach number, it offers the flexibility to have the condition number increase by a factor 2 in order to reduce flow-angle sensitivity. The matrix has also caused a break-through in the formulation of genuinely multi-dimensional fluctuation-splitting schemes, after it was discovered that it yields the proper decoupling of the acoustic from the convective components present in the Euler equations.

Robustness of Euler calculations in the presence of preconditioning has been an issue during the entire contract period, but it appears that the worst problems are over, now that the stagnation-point instability has been properly understood. This instability is caused in part by the lack of orthogonality of certain matrix eigenvectors, resulting in a transient up-swinging of numerical errors.

The Euler preconditioning has been embedded in a Navier-Stokes preconditioning through the use of a simple Jacobi block to account for the dissipative terms. There is still a robustness issue in the limit of vanishing cell Reynolds-number. The inclusion of a convective turbulence-transport equation appears to be easily accounted for in the

preconditioning matrix, in the same way as is done for the extra continuity equations needed in describing multi-species reacting flow.

All results not included in Lynn's thesis will be presented in the doctoral thesis of Dohyung Lee, which is expected to be defended in the Winter Term of 1996.

When reviewing progress in CFD over the past three years, it is observed that the introduction of the Van Leer-Lee-Roe preconditioning matrix at the 10th AIAA CFD Conference in June 1991 set a new CFD trend. Local preconditioning matrices for the low-speed flow regime had been introduced by Turkel from 1984 onwards, and were used extensively by Merkle et al. at Pennsylvania State University, but their use did not spread further. At present there is a rapidly growing appreciation of local preconditioning, both in the USA and Europe (Netherlands, Belgium, Germany, UK, France), probably because the locality of this convergence-acceleration technique combines well with parallel computer architectures.

4 Future research

To make our type of local preconditioning a robust technique, as robust as the traditional point-Jacobi preconditioning, and suited for non-expert users, some work still needs to be done:

a. Testing the robustness of the stagnation-point modifications under a wide range of circumstances, i. e. Mach numbers, flow angles, cell aspect-ratios and cell Reynolds-numbers;

b. Optimizing the smoothing of matrix elements in the sonic-point singulatity;

c. Overcoming the loss of robustness for very low cell Reynolds numbers.

Among new uses of local preconditioning awaiting exploration are:

- Local preconditioning for atmospheric problems, eliminating stiffness due to acoustic and gravitational waves;
- Preconditioning for magneto-hydrodynamics. eliminating stiffness due to magneto-acousic and Alfvén waves;
- Local preconditioning expanded hydrodynamic equation systems derived from the collisional Boltzmann equation (a continuation of the work under the current augmentation grant). This has applications in upper-atmosphere and plasma flows as well as micro-manufacturing and solid-state modeling.

We plan to submit a new research proposal addressing these topics in the near future.

Appendix A

Paper AIAA 1654-95

Appendix B

Paper AIAA 1667-95

Appendix A
AIAA Paper 95-1654 CP

Local preconditioning in a stagnation point

Bram van Leer* Lisa Mesaros †

W. M. Keck Foundation Laboratory for Computational Fluid Dynamics
Department of Aerospace Engineering
University of Michigan, Ann Arbor, MI 48109-2118

Chang-Hsien Tai‡

Department of Mechanical Engineering
Chung-Cheng Institute of Technology, Ta-Hsi, Taiwan 33509

and

Eli Turkel§

School of Mathematical Sciences
Tel-Aviv University, Ramat-Aviv, Israel

Abstract

Local preconditioning yields desirable effects such as convergence acceleration and preservation of accuracy in the incompressible limit, but these come at the expense of robustness. Current research focuses on making the various preconditioned Euler discretizations that have been developed more reliable near flow singularities such as sonic and stagnation points. In this report we discuss the loss of stability in computing stagnating flow with the symmetric Van Leer-Lee-Roe preconditioning, and do an exhaustive search for modifications of the matrix (for low Mach numbers) by which the instability can be avoided. Some

*Fellow AIAA.
†Member AIAA.
‡Member AIAA.
§Member AIAA.

numerical support regarding the effectiveness of these modifications is presented.

1 Introduction

Local preconditioning can be used to make the time-dependent Euler equations more suited to the numerical computation of steady solutions. In the following analysis preconditioning is accomplished by multiplying the spatial differential operator by a locally evaluated matrix. First, let us introduce some notation.

The two-dimensional Euler equations will be written as

$$\frac{\partial U}{\partial t} + A(U)\frac{\partial U}{\partial x} + B(U)\frac{\partial U}{\partial y} = 0, \quad (1)$$

where the state variables are defined differentially:

$$dU = (\frac{dp}{\rho a}, du, dv, dS)^T; \quad (2)$$

a denotes sound speed, S entropy. These variables have the property of symmetrizing the Euler equations:

$$A(U) = \begin{pmatrix} u & a & 0 & 0 \\ a & u & 0 & 0 \\ 0 & 0 & u & 0 \\ 0 & 0 & 0 & u \end{pmatrix}, \quad (3)$$

$$B(U) = \begin{pmatrix} v & a & 0 & 0 \\ a & v & 0 & 0 \\ 0 & 0 & v & 0 \\ 0 & 0 & 0 & v \end{pmatrix}. \quad (4)$$

Much of the analysis can be done assuming that the fluid moves in the positive x-direction, so that u equals the full flow speed q, and v vanishes (but not its derivatives). The Euler equations then read

$$\frac{\partial U}{\partial t} + a\begin{pmatrix} M & 1 & 0 & 0 \\ 1 & M & 0 & 0 \\ 0 & 0 & M & 0 \\ 0 & 0 & 0 & M \end{pmatrix}\frac{\partial U}{\partial x} + a\begin{pmatrix} 0 & 0 & 1 & 0 \\ 0 & 0 & 0 & 0 \\ 1 & 0 & 0 & 0 \\ 0 & 0 & 0 & 0 \end{pmatrix}\frac{\partial U}{\partial y} = 0, \quad (5)$$

where M is the Mach number.

The preconditioned Euler equations read

$$\frac{\partial U}{\partial t} + P(U)\left(A(U)\frac{\partial U}{\partial x} + B(U)\frac{\partial U}{\partial y}\right) = 0, \quad (6)$$

where $P(U)$ is a positive definite matrix. If P is symmetric, so is P^{-1}, and the system

$$P(U)^{-1}\frac{\partial U}{\partial t} + A(U)\frac{\partial U}{\partial x} + B(U)\frac{\partial U}{\partial y} = 0 \quad (7)$$

is symmetric, just as the original system. If P is not symmetric, it is desirable that the preconditioned system be *symmetrizable*; th puts certain constraints on the elements of P [1].

In the course of our research on local preconditioning of the Euler equations the following computational benefits have been identified.

1. Local preconditioning can be designed to remove the stiffness of the system of equations caused by the range of the characteristic speeds, thus improving the convergence rate of any discrete marching scheme [2].

2. It then makes the system of equations behave more like a scalar equation, which is advantageous in designing and applying additional convergence-acceleration techniques [3].

3. It generates spatial discretizations that may retain their accuracy at low Mach number, in contrast to standard discretizations [4, 5, 6].

4. It can be designed to decouple the acoustic equations from the convective equations, allowing genuinely multidimensional discretizations [1]

These desirable properties come at the expense of robustness. Current research focuses on making the various preconditioned Euler discretizations that have been developed more reliable near flow singularities, such as sonic and stagnation points. In this report we describe the loss of stability in computing stagnating flow with the symmetric Van Leer-Lee-Roe preconditioning [2], and how to overcome it by modifying the matrix for low Mach numbers.

2 Sensitivity to flow angle

With the choice of flow variables (2) and the flow aligned with the x-axis, the Van Leer-Lee-Roe preconditioning matrix for subsonic flow ($M < 1$) takes the form

$$P(U) = \begin{pmatrix} \frac{M^2}{\beta} & -\frac{M}{\beta} & 0 & 0 \\ -\frac{M}{\beta} & \frac{1}{\beta}+1 & 0 & 0 \\ 0 & 0 & \beta & 0 \\ 0 & 0 & 0 & 1 \end{pmatrix}, \quad (8)$$

where $\beta = \sqrt{1-M^2}$. Use of this matrix reduces the condition number of the characteristic speeds from $(M+1)/\min(1-M, M)$ to $1/\beta$. For an appreciation of the stability problem near a stagnation point we must obtain the form of the matrix valid for any flow angle ϕ, i. e.

$$P_\phi(U) = R_\phi^{-1}(U) P(U) R_\phi(U) \quad (9)$$

with

$$R_\phi(U) = \begin{pmatrix} 1 & 0 & 0 & 0 \\ 0 & \cos\phi & \sin\phi & 0 \\ 0 & -\sin\phi & \cos\phi & 0 \\ 0 & 0 & 0 & 1 \end{pmatrix}; \quad (10)$$

this yields Equation (11). It is seen that this matrix remains sensitive to the flow angle when the Mach number decreases toward zero, because its inner elements (2,2), (2,3), (3,2) and (3,3), which depend on ϕ, remain $\mathcal{O}(1)$. In this case numerical perturbations to u and v that are small in absolute value may not be small when compared to the values of u and v, causing $\mathcal{O}(1)$ variations in ϕ and the four matrix elements. This sensitivity can be traced back to the fact that the elements (2,2) and (3,3) of P are not equal. It is believed to contribute to the numerical instability near a stagnation point, often experienced

$$P_\phi(U) = \begin{pmatrix} \frac{M^2}{\beta} & -\frac{M}{\beta}\cos\phi & -\frac{M}{\beta}\sin\phi & 0 \\ -\frac{M}{\beta}\cos\phi & \left(\frac{1}{\beta}+1\right)\cos^2\phi + \beta\sin^2\phi & \left(\frac{1}{\beta}+1-\beta\right)\sin\phi\cos\phi & 0 \\ -\frac{M}{\beta}\sin\phi & \left(\frac{1}{\beta}+1-\beta\right)\sin\phi\cos\phi & \left(\frac{1}{\beta}+1\right)\sin^2\phi + \beta\cos^2\phi & 0 \\ 0 & 0 & 0 & 1 \end{pmatrix}. \qquad (11)$$

with conservative upwind Euler schemes that include the above matrix. In such schemes the artificial-dissipation matrices [2] used in the streamwise and normal fluxes are

$$P^{-1}|PA|, \quad P^{-1}|PB|, \qquad (12)$$

rather than $|A|$ and $|B|$, as in the original upwind schemes. In the update the spatial residual in each cell is multiplied by the cell-centered value of P_ϕ, creating products

$$(P_\phi)_{\text{center}}(P_\phi^{-1})_{\text{face}} \qquad (13)$$

that may vary erratically near a stagnation point and deviate appreciably from the values elsewhere in smooth flow, which should be close to the identity matrix. In a study by D. Lee [7] a uniform slow flow perturbed by rotating the velocity in one cell by 90° became unstable when advanced in time by an explicit first-order upwind scheme preconditioned as above. The instability could be forestalled, but not avoided, by taking smaller time steps. A similar behavior was found when simulating an isolated stagnation region. Andrew Godfrey reports [8] that implicit time integration can suppress the instability if the grid used is not too fine.

Besides flow-angle sensitivity there is a more obvious problem: the vanishing of several elements of the matrix (8) near a stagnation point, especially the (1,1) element. In practice it has been found necessary to bound the value of M away from zero in these el ments, e.g. replace it by

$$\bar{M} = \min(0.1M_\infty, 0.1). \qquad (14)$$

For conservative schemes, which include the inverse of P in the artificial-viscosity coefficients (12), such a procedure clearly makes sense [2]; less obvious is it that nonconservative schemes also increase in robustness by this measure. It appears that use of the actual value of M makes the pressure correction allowed by the preconditioned equations so small that the flow does not properly turn in the stagnation region.

Returning to the subject of flow-angle sensitiviy, an indication that this indeed contributes to stagnation-region instability was found by Tai [9], who obtained stability and convergence by using a *nonconservative* version of the preconditioned schemes, in which the product (13) is omitted. Furthermore, preconditioned schemes based on Turkel's [10] matrix, whether or not in conservation form, do not exhibit the instability. This can be readily understood from the structure of this matrix; for streamwise x-axis and sufficiently

small Mach number it reduces to

$$P_T(U) = \begin{pmatrix} M^2 & 0 & 0 & 0 \\ -M & 1 & 0 & 0 \\ 0 & 0 & 1 & 0 \\ 0 & 0 & 0 & 1 \end{pmatrix}, \qquad (15)$$

which is seen to be lower triangular. The elements (2,2) and (3,3) of this matrix are equal; in consequence, its version for arbitrary flow angle,

$$P_T\phi(U) = \begin{pmatrix} M^2 & 0 & 0 & 0 \\ -M\cos\phi & 1 & 0 & 0 \\ -M\sin\phi & 0 & 1 & 0 \\ 0 & 0 & 0 & 1 \end{pmatrix} \qquad (16)$$

is well behaved for $M \to 0$. It is possible to extend the matrix (15) so as to yield the minimum possible spread of the characteristic speeds throughout the subsonic domain, without giving up its lower-triangular structure. The resulting matrix is

$$P_T(U) = \begin{pmatrix} \frac{M^2}{\beta} & 0 & 0 & 0 \\ -\frac{M}{\beta} & 1 & 0 & 0 \\ 0 & 0 & \beta & 0 \\ 0 & 0 & 0 & 1 \end{pmatrix}. \qquad (17)$$

While it does not suffer from flow-angle sensitivity, the preconditioning matrix (15) has another problem: it lies at the limit of admissibility. Turkel [10] found that the preconditioned system of equations is no longer symmetrizable, implying, among other things, that it no longer has an entropy condition [11] distinguishing between physical and nonphysical admissible solutions. An arbitrarily small perturbation of the matrix, though, can make the system symmetrizable again. Indeed, it has been pointed out by Turkel that the matrix (15) itself does not work in practice, but the perturbed matrix

$$P_T\phi(U) = \begin{pmatrix} (1+\epsilon)M^2 & 0 & 0 & 0 \\ -M & 1 & 0 & 0 \\ 0 & 0 & 1 & 0 \\ 0 & 0 & 0 & 1 \end{pmatrix}, \qquad (18)$$

with $\epsilon > 0$ for symmetrizability, does speed up numerical convergence.

It is not *a priori* clear that, in the limit of $M \to 0$, the matrix (15) is the only optimal preconditioner with the property that its (2,2) and (3,3) element are equal. It would be preferable if an optimal matrix existed closer to Van Leer's, i. e. more nearly symmetric. To find out about this, the best one can do is to examine all possible matrices. This is actually done in the next section.

3 Analysis in the incompressible limit

Since the stability problem with the symmetric preconditioner occurs only for small M, it is advantageous to base the further analysis on the incompressible Euler equations, at least as a start. This means the reference Mach number, e. g. M_∞, is assumed to be small; the flow velocity itself is now regarded to be $O(1)$.

The Euler equations for incompressible flow are made hyperbolic through "artificial compressibility" [12], implemented by adding a time derivative of pressure to the elliptic con-

tinuity equation:

$$\frac{p_t}{\rho \bar{a}^2} + u_x + v_y = 0, \quad (19)$$

$$u_t + uu_x + vu_y + \frac{p_x}{\rho} = 0, \quad (20)$$

$$v_t + uv_x + vv_y + \frac{p_x}{\rho} = 0, \quad (21)$$

where $\bar{a}$ is now a constant artificial speed of sound, and ρ is also a constant; the entropy equation drops out. Using otherwise the same variables and coordinates as before, the equations can be written as

$$\frac{\partial U}{\partial t} + \bar{a} \begin{pmatrix} 0 & 1 & 0 \\ 1 & m & 0 \\ 0 & 0 & m \end{pmatrix} \frac{\partial U}{\partial x} \quad (22)$$

$$+ \bar{a} \begin{pmatrix} 0 & 0 & 1 \\ 0 & 0 & 0 \\ 1 & 0 & 0 \end{pmatrix} \frac{\partial U}{\partial y} = 0, \quad (23)$$

where $m = u/\bar{a}$ is the artificial Mach number, of magnitude $O(1)$. Next we precondition this system with the most general matrix possible:

$$\bar{P}(U) = \begin{pmatrix} a & D & E \\ d & b & F \\ e & f & c \end{pmatrix}; \quad (24)$$

note that a is a free parameter and has nothing to do with the speed of sound. For an arbitrary flow angle this matrix transforms into $\bar{P}_\phi(U)$, given in Equation (25). Consider first the 2×2 block of elements (2,2), (2,3), (3,2), (3,3). In order to avoid too strong a dependence on the flow angle near a stagnation point, i. e. for $m \to 0$, both $b - c$ and $f + F$ must either equal zero or vanish sufficiently rapidly with m. Thus, b, c, f and F can all be $O(1)$, but b and c must be equal or close to equal, while f and F must be opposite or close to opposite. For the present purpose it therefore suffices to assume

$$b = c; \quad (26)$$

$$F = -f; \quad (27)$$

it is instructive to carry b and c along as separate parameters as long as possible, since this allows us to link the Van Leer and Turkel m trices.

3.1 Optimal asymmetric matrices

Next we study the characteristic speeds of the preconditioned equations, i. e. the propagation speeds of the plane-wave solutions admitted by these equations. If we denote the propagation direction by the angle θ, the speeds are the eigenvalues of the matrix

$$\bar{P}(\bar{A}\cos\theta + \bar{B}\sin\theta). \quad (2$$

Using the coefficient matrices from (23) and the general preconditioning (24), the eigenvalue equation becomes (29). or

$$-\lambda^3 + K_2\lambda^2 - K_1\lambda + K_0 = 0, \quad (30)$$

with

$$\begin{aligned} K_2 &= [d + D + bm + cm]\cos\theta \\ &+ (e + E)\sin\theta, \quad (31) \\ K_1 &= [(d + D + bm)cm - ab + dD \\ &- eFm - fEm - fFm^2]\cos^2\theta \end{aligned}$$

$$\begin{pmatrix} a & D\cos\phi - E\sin\phi & D\sin\phi + E\cos\phi \\ d\cos\phi - e\sin\phi & b\cos^2\phi + c\sin^2\phi - (f+F)\sin\phi\cos\phi & (b-c)\sin\phi\cos\phi - f\sin^2\phi + F\cos^2\phi \\ d\sin\phi + e\sin\phi & (b-c)\sin\phi\cos\phi + f\cos^2\phi - F\sin^2\phi & b\sin^2\phi + c\cos^2\phi + (f+F)\sin\phi\cos\phi \end{pmatrix}. \tag{25}$$

$$\det \begin{pmatrix} D\cos\theta + E\sin\theta - \lambda & (a+Dm)\cos\theta & Em\cos\theta + a\sin\theta \\ b\cos\theta + F\sin\theta & (d+bm)\cos\theta - \lambda & Fm\cos\theta + d\sin\theta \\ f\cos\theta + c\sin\theta & (e+fm)\cos\theta & cm\cos\theta + e\sin\theta - \lambda \end{pmatrix} = 0. \tag{29}$$

$$\begin{aligned} &+ (-ac + eE)\sin^2\theta \\ &+ [(f+F)a + (e+E)bm + (E - fm)d \\ &+ (e - Fm)D]\sin\theta\cos\theta, \qquad (32) \\ K_0 &= -m\cos\theta \det P. \qquad (33) \end{aligned}$$

If P were an optimal preconditioner, all wave speeds would turn out equal, i. e., the acoustic waves would propagate at the flow speed in all directions. This suggests the following target equation for the λ's:

$$(m\cos\theta - \lambda)(\lambda^2 - m^2) = 0, \tag{34}$$

or

$$-\lambda^3 + \lambda^2 m\cos\theta + \lambda m^2 - m^3\cos\theta = 0. \tag{35}$$

Comparing the target equation to the general equation leads to 6 constraints (two from K_2, three from K_1 and one from K_0) on the 9 parameters a, b, c, d, e, D, E. One therefore would hope to find a one-parameter family of matrices satisfying the additional constraints (26) and (27).

Starting with the $\sin\theta$-term in K_2, we see that

$$e + E = 0; \tag{36}$$

it does not bode well for symmetrizability that both pairs (e, E) and (f, F) must be *anti*symmetric. Using both (27) and (36), the remaining conditions reduce to

$$d + D + bm = m(1 - c) \tag{37}$$

from K_2,

$$\begin{aligned} &(d + D + bm)cm - ab + dD \\ &+(e + fm)^2 - e^2 = -m^2, \qquad (38) \end{aligned}$$

$$ac + e^2 = m^2 \tag{39}$$

and

$$(D - d)(e + Fm) = 0 \tag{40}$$

from K_1, and

$$\begin{aligned} &(ab - dD)c + af^2 + be^2 \\ &-(d + D)ef = m^2 \qquad (41) \end{aligned}$$

from K_0.

Considering Eq. (40) it appears we have two choices:

$$e + fm = 0, \tag{42}$$

which also means

$$E + Fm = 0, \tag{43}$$

or

$$d = D. \tag{44}$$

Pursuing first the choice $e + fm = 0$ we find that Eqs. (37,38,39,41), while up to cubic in the unknown parameters, allow elimination of a, b, d and D. The result is a relation between c and f,

$$(c^2 + f^2 - 1)(c^2 + f^2 - c) = 0, \tag{45}$$

meaning either

$$f^2 = 1 - c^2 \tag{46}$$

or

$$f^2 = c(1 - c). \tag{47}$$

The first choice, Eq. (46), suggests interpreting c and f as $\cos\psi$ and $\sin\psi$, where ψ is an arbitrary angle; it leads to the following two-parameter matrix (or its transposed) satisfying all previous constraints except (26):

$$\bar{P}(U) = \begin{pmatrix} cm^2 & (1-b)m & \pm\sqrt{1-c^2}m \\ -cm & b & \mp\sqrt{1-c^2} \\ \mp\sqrt{1-c^2}m & \pm\sqrt{1-c^2} & c \end{pmatrix} \tag{48}$$

This general formula includes the Turkel matrix ($b = c = 1$) and the Van Leer matrix ($b = 2,\ c = 1$); we shall discuss its properties further below.

The second choice, Eq. (47), complicates the algebra; to simplify the analysis we have to implement the constraint (26) right away. With $b = c$ we obtain the one-parameter matrix (49). In this matrix we may replace c by $\frac{1}{2}(1 + \cos\phi)$, whereupon f becomes $\frac{1}{2}\sin\psi$. Turkel's matrix again is obtained for $c = 1$.

Going back to Eq. (40), we still have to follow its second branch Eq. (44), which makes the pair (d, D) symmetric. Again the algebra becomes complicated, forcing us to insert $b = c$ right away. When eliminating a and d from the remaining equations it turns out that c also drops out, yielding

$$(e + fm)^2 = -\frac{1}{4}m^2, \tag{50}$$

which can not be satisfied by real e and f. Apparently, the equality of d and D excludes the equality of b and c.

Upon inspecting the yield of the above analysis, *viz.* matrices (48) and (49), it appears that equality of b and c, with c always less than 1, makes these matrices even more skewed than Turkel's matrix, and therefore further away from producing a symmetrizable preconditioned system. The extra freedom offered by the parameters e and f, hitherto not included in any analysis, does not lead to more preferable matrices, and we shall henceforth assume these to be zero. For future reference we repeat the matrix (48), inserting $c = 1$, which eliminates e and f:

$$\bar{P}(U) = \begin{pmatrix} m^2 & (1-b)m & 0 \\ -m & b & 0 \\ 0 & 0 & 1 \end{pmatrix}; \tag{51}$$

this is the incompressible version of the following matrix valid for subsonic compressible flow:

$$P(U) = \begin{pmatrix} \frac{M^2}{\beta} & (1-b)\frac{M}{\beta} & 0 & 0 \\ -\frac{M}{\beta} & b & 0 & 0 \\ 0 & 0 & \beta & 0 \\ 0 & 0 & 0 & 1 \end{pmatrix}. \tag{52}$$

$$\tilde{P}(U) = \begin{pmatrix} \left(c + \frac{1}{c} - 1\right) m^2 & (1-c)m & \pm\sqrt{c(1-c)}m \\ -cm & c & \mp\sqrt{c(1-c)} \\ \mp\sqrt{c(1-c)}m & \pm\sqrt{c(1-c)} & c \end{pmatrix}. \tag{49}$$

One choice of $b(M)$ that links the Turkel matrix for $M = 0$ to the Van Leer matrix for greater subsonic values of M is

$$b(M) = \frac{1}{\beta} + 1 - \beta^r, \tag{53}$$

where r is some positive power, e. g. $r = 2$.

3.2 Sub-optimal symmetric matrices

We are now left with two possible strategies of fighting the stagnation-point instability:

1. use a matrix of the form (52), with $b(M)$ varying with the Mach number from

$$b(0) = 1 \tag{54}$$

to

$$b(1) = 2. \tag{55}$$

2. develop a one-parameter family of *sub*-optimal symmetric matrices satisfying the same conditions (54) and (55).

In this section we shall pursue the second possibility. Preserving symmetry, even if it means giving up optimality, is valuable because it is cruicial in coding update schemes based on multidimensional fluctuation splitting [13]; see further Section 4 on numerical results.

The family of matrices of the form

$$P(U) = \begin{pmatrix} a & d & 0 & 0 \\ d & b & 0 & 0 \\ 0 & 0 & c & 0 \\ 0 & 0 & 0 & 1 \end{pmatrix}; \tag{56}$$

has been analyzed in great detail by Wen-Tzong Lee[4]. From this analysis we conclude that the following variation on the Van Leer matrix (8) will offer sufficient freedom:

$$P(U) = \begin{pmatrix} C_1\frac{M^2}{\beta} & -C_1\frac{M}{\beta} & 0 & 0 \\ -C_1\frac{M}{\beta} & C_1\frac{1}{\beta} + C_2 & 0 & 0 \\ 0 & 0 & C_4\beta & 0 \\ 0 & 0 & 0 & C_3 \end{pmatrix}. \tag{57}$$

With this choice of preconditioning, the plane-wave speeds $\lambda(\theta)$ follow from the equation

$$\begin{aligned} &(C_2 M\cos\theta - \lambda)(C_3 M\cos\theta - \lambda) \times \\ &\{\lambda^2 + \lambda M(C_4 - C_2)\cos\theta \\ &-C_1 C_4 M^2[(1-M^2)\cos^2\theta + \sin^2\theta]\} = 0; \end{aligned} \tag{58}$$

for $\theta = 0$ we have in particular:

$$\begin{aligned} &(C_1\beta M + \lambda)(C_2 M - \lambda)(C_3 M - \lambda) \times \\ &(\lambda^2 - C_4\beta M) = 0. \end{aligned} \tag{59}$$

It is seen that the coefficients C_1, C_2, C_3 and C_4 scale, respectively, the backward acoustic speed, the shear-convection speed, the

entropy-convection speed and the forward acoustic speed. The acoustic wave front, which is the envelope of the graph of the acoustic plane waves, is an ellipse with equation

$$\left(\frac{x-\frac{1}{2}(C_4-C_1)\beta M}{\frac{1}{2}(C_1+C_4)}\right)^2+\left(\frac{y}{\sqrt{C_1C_4}M}\right)^2=1. \tag{60}$$

In order to make the elements b and c of P equal for $M \to 0$, we must satisfy

$$\frac{C_1(M)}{\beta}+C_2(M)=C_4(M)\beta \tag{61}$$

for $M \to 0$, or simply

$$C_1(0)+C_2(0)=C_4(0). \tag{62}$$

This means that both the backward acoustic speed and the shear-convection speed must be reduced in magnitude with respect to the forward acoustic speed. The best condition number results when the backward acoustic and shear speeds are equal in magnitude, i. e.

$$C_1(0)=C_2(0)=\frac{1}{2}C_4(0). \tag{63}$$

In order to keep the normalization that the largest characteristic speed equals the flow speed, we take $C_4(0)$ to be 1. which makes both $C_1(0)$ and C_2 equal to $\frac{1}{2}$. Since the three coefficients all should tend to 1 for the larger subsonic values of M, there is no reason to let C_4 differ from 1 for any Mach number, nor C_1 from C_2. Our final choice therefore is

$$C_1(M) = C_2(M)=\alpha(M), \tag{64}$$

$$\alpha(0) = \frac{1}{2}, \tag{65}$$

$$\alpha(1) = 1, \tag{66}$$

$$C_4(M) \equiv 1. \tag{67}$$

One question remains: should the entropy-convection speed be re-scaled, or may it remain equal to the flow speed? There is some evidence that the entropy speed better equal the shear speed: in one of our airfoil calculations an instabilty encountered at the far-field boundary could be suppressed by lowering th entropy speed to the shear-speed value. A possible explanation is that for the *preconditioned* system of equations the quantity convected besides entropy is not shear strength but actually is the total enthalpy for an isentropic process. If entropy and isentropic total enthalpy are convected at different speeds their values may get out of sync, feeding an instability. If this explanation is correct, another way of preventing the instability is to add a multiple of the entropy-convection equation to the other convection equation, so that a convection equation results for the full t(tal enthalpy, not subject to a speed restriction. However this may be, for the time being we shall take the enthalpy- and entropy-convection speeds equal, i. e.,

$$C_3(M)=\alpha(M). \tag{68}$$

Our sub-optimal, symmetric preconditioner thus becomes

$$P(U)=\begin{pmatrix} \alpha\frac{M^2}{\beta} & -\alpha\frac{M}{\beta} & 0 & 0 \\ -\alpha\frac{M}{\beta} & \alpha\left(\frac{1}{\beta}+1\right) & 0 & 0 \\ 0 & 0 & \beta & 0 \\ 0 & 0 & 0 & \alpha \end{pmatrix}. \tag{69}$$

For our numerical experiments we chose

$$\alpha = \frac{1}{2}, \quad 0 \le M \le \frac{1}{3}, \tag{70}$$

$$\alpha = \frac{3}{4}\left\{1 + 3\left(M - \frac{1}{2}\right)\left[1 - 12\left(M - \frac{1}{2}\right)^2\right]\right\}, \quad \frac{1}{3} < M < \frac{2}{3}, \tag{71}$$

$$\alpha = 1, \quad \frac{2}{3} \le M < 1, \tag{72}$$

a continuously differentiable function which uses a cubic to switch between the two plateau values.

4 Numerical results

We experimented with both preconditioners, the asymmetric matrix (52) and the symmetric matrix (69); the results can be summarized as follows.

1. Both new asymmetric and symmetric preconditioners made it possible to converge with a conservative upwind code (structured grid, cell-average update) to steady solutions for low-speed flow cases in which the original Van Leer-Lee-Roe preconditioner (8) would lead to instability or failure to converge. The symmetric preconditioner was the most robust of the two, allowing the use of lower Mach numbers and finer grids, and giving faster convergence.

2. Even the better preconditioner of the two can hardly be called robust: it still needed special handling in order to avoid blow-up for an impulsively started flow field, in addition to the mandatory downward limiting of the M-values in P [2].

3. Surprisingly, the symmetric preconditioner greatly improved a *nonconservative* flow code, namely, the unstructured cell-vertex code developed by Mesaros [13] on the basis of fluctuation-splitting ideas. The equations used are those found after preconditioning the Euler equations with the Van Leer-Lee-Roe preconditioning, which neatly separates the acoustic equations (a pair of time-dependent Cauchy-Riemann equations) from the two convection equations (one for the isentropic total enthalpy and one for entropy). The convection eqations are updated by a state-of-the-art multidimensional upwind advection scheme, the acoustic equations are by a cell-vertex distribution scheme similar to that of Ni [14]. The procedure previously failed to converge for airfoil flows at lower inflow Mach-numbers, with the strongest indeterminacy occurring in the leading-edge stagnation region. The sub-optimal symmetric preconditioner decouples the equations just as the optimal one, and made it possible to achieve accurate converged results for arbitrarily low M_∞ on a fine grid, without any further special measures.

Figure 2 shows Mach contours of the steady solutions obtained for flow over a NACA 0012 at zero angle of attack, for inflow Mach numbers of 0.1 (top) and 0.01 (bottom). The grid has 131 nodes on

the body, strongly clustered at the leading edge. The two solutions are practically indistinguishable and, as shown in Figure 1, have identical convergence histories, except for a scale difference of a factor 100 between the residuals. The solutions are of high quality, as evidenced by the low drag coefficient of 0.0002 obtained in both cases.

4. When changing to a conservative update scheme Mesaros' code lost robustness for low-speed flows, showing problems similar to those experienced with the cell-average-based finite-volume code. In particular, the code would not tolerate impulsive-start conditions; the nonconservative version of the code had to be used to get through the initial transients. Alternatively, increasing the artificial dissipation in the acoustic distribution scheme could be used to stabilize the scheme initially. It was further observed that the lower bound on M in the elements of P had to be raised in the conservative code.

5. Another conservative cell-vertex code [15], though, seemed to draw no benefit at all from the modified preconditioner: it performed as well without as with the modification. This code was developed by D. Darmofal for the study of Euler preconditioners, in particular, the effect of a preconditioner on the eigen*vector* structure of the equations. The scheme implemented was Barth's [16], which uses cell-vertex values to define Riemann problems at the faces of co-volumes. Darmofal found that the problems of instability or nonconvergence near a stagnation point are solely caused by certain acoustic eigenvectors becoming parallel for $M \to 0$, and that bounding M away from zero in the (1,1) element of P solves these problems. So far the following combinations of preconditioners and numerical flux functions have been tested:

   - Turkel preconditioning with scalar artificial viscosity;
   - Turkel preconditioning with matrix viscosity (upwind differencing);
   - Van Leer preconditioning with scalar artificial viscosity.

   Although it is still to early to draw a firm conclusion, it seems that at least this particular kind of cell-vertex code can easily be made robust, and that any modification of the preconditioning should be motivated by orthogonalizing eigenvectors, rather than relaxing the condition number of eigenvalues.

5 Conclusions

In the present study we deveoped a modified preconditioner that reduces the sensitivity of the preconditioned flow equations to the flow angle in a stagnation region. This dramatically improves the stability and convergence of

at least one flow code, a nonconservative cell-vertex code described elsewhere in this volume [13]. The effect on certain conservative codes is not impressive, while yet another conservative code, also described elsewhere in this volume [15], does not seem to need the modification at all. All preconditioners need some downward limiting of the value of the Mach number; its beneficial effect, according to Darmofal and Schmid [15], is mostly to prevent the eigenvectors of certain acoustic waves to become parallel.

Acknowledgement
The research reported in this paper was done while the authors were in residence at ICASE, NASA Langley Research Center, Hampton, VA, in the summer of 1995.

References

[1] E. Turkel and P. L. Roe, "Decomposition of the Euler equations." ICASE Report, in preparation, 1994.

[2] B. van Leer, W. T. Lee, and P. L. Roe, "Characteristic time-stepping or local preconditioning of the Euler equations," in *AIAA 10th Computational Fluid Dynamics Conference*, 1991.

[3] J. F. Lynn and B. van Leer, "Multistage schemes for the Euler and Navier-Stokes equations with optimal smoothing," AIAA Paper 93-3355-CP, 1993.

[4] W.-T. Lee, *Local Preconditioning of the Euler Equations.* PhD thesis, University of Michigan, 1991.

[5] A. G. Godfrey, *Topics on Spatially Accurate Methods and Preconditioning for the Navier-Stokes Equations with Finite-Rate Chemistry.* PhD thesis, VPI & SU, 1992.

[6] E. Turkel, A. Fiterman, and B. van Leer, "Preconditioning and the limit to the incompressible flow equations." ICASE Report 93-42, 1993.

[7] D. Lee, *Local Preconditioning of the Euler and Navier-StokesEquations.* PhD thesis, University of Michigan, 1994. In preparation.

[8] A. G. Godfrey. Private Communication, 1994.

[9] C.-H. Tai, "Calculation of viscous flow over a projectile." Technical Report, Department of Mechanical Engineering, Chung-Cheng Institute of Technology, 1993.

[10] E. Turkel, "Preconditioned methods for solving the incompressible and low speed compressible equations," *Journal of Computational Physics*, vol. 72, 1987.

[11] S. K. Godunov, "An interesting class of quasilinear systems," *Dokl. Akad. Nauk SSSR*, vol. 139, pp. 521–523, 1961.

[12] A. J. Chorin, "A numerical method for solving incompressible viscous flow problems," *Journal of Computional Physics*, vol. 2, 1967.

[13] L. M. Mesaros and P. L. Roe, "Multi-dimensional fluctuation-splitting schemes based on decomposition methods," AIAA Paper 95-1699, 1995.

[14] R. H. Ni, "A multiple-grid scheme for solving the Euler equations," *AIAA Journal*, vol. 20, 1981.

[15] D. L. Darmofal and P. J. Schmid, "The importance of eigenvectors for local preconditioning of the Euler equations," AIAA Paper 95-1655, 1995.

[16] T. J. Barth and D. C. Jespersen, "The design and application of upwind schemes on unstructured meshes," AIAA Paper 89-0366, 1989.

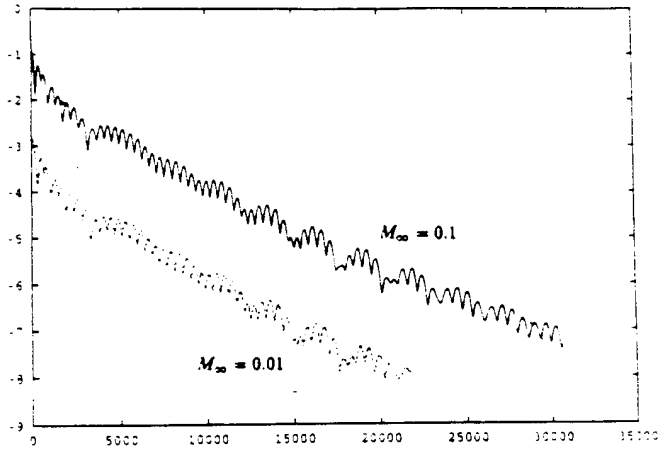

Figure 1: Residual histories for the calculations of the steady solutions shown in Figure 2.

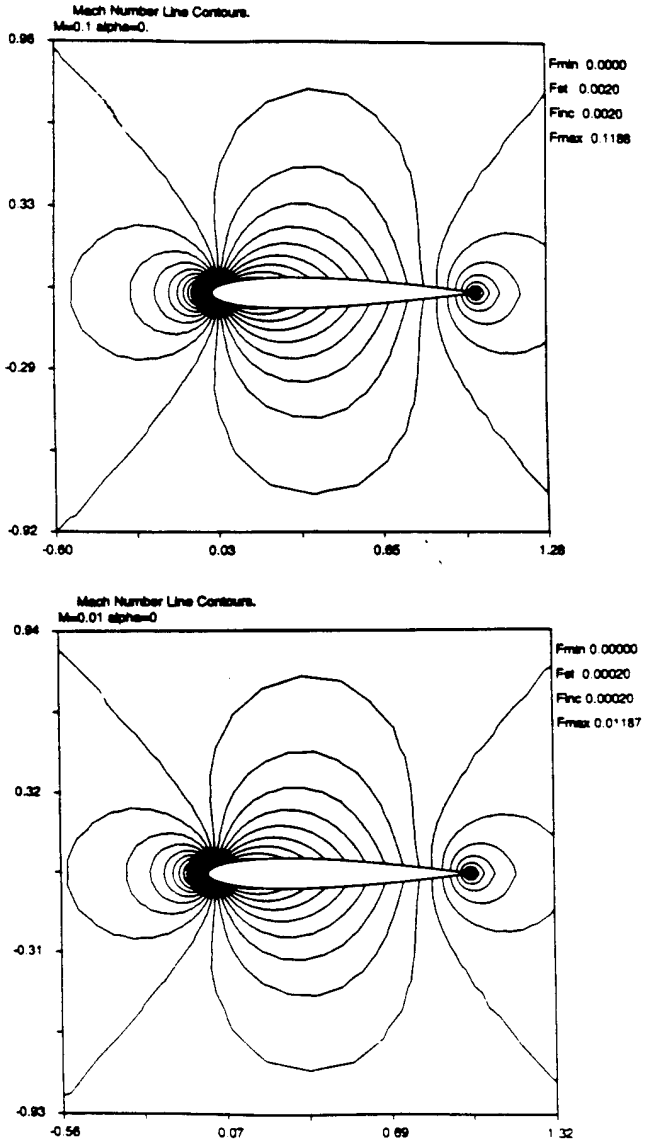

Figure 2: Mach contours for flow over a NACA 0012 at zero angle of attack; for a description of code and grid see the main text. Top: $M_\infty = 0.1$, bottom: $M_\infty = 0.01$.

APPENDIX B
AIAA Paper 95-1667 CP

A Semi-Coarsened Multigrid Solver for the Euler and Navier-Stokes Equations with Local Preconditioning

John F. Lynn* and **Bram van Leer†**

W. M. Keck Foundation Laboratory for Computational Fluid Dynamics,

Department of Aerospace Engineering, The University of Michigan,

Ann Arbor, MI 48109-2118

Abstract

An optimization formulation is described for multi-stage schemes based on the hi-hi high-frequency content in the Fourier footprint of the preconditioned spatial operator. These coefficients, when used in conjunction with semi-coarsened multigrid and local preconditioning provide a fast and robust method for achieving steady-state Euler solutions. Multigrid speed-ups of 3-4 times are observed when using local preconditioning as compared to local time-stepping. The extension to Navier-Stokes operators is also described.

1 Introduction

Explicit marching schemes are commonly used as multigrid relaxation schemes when solving the Euler and Navier-Stokes equations. These schemes must feature effective high-frequency damping in order to be suited for use in multigrid marching. Multi-stage schemes provide the flexibility to achieve the desired smoothing properties. True multigrid convergence rates can only result with multi-stage relaxation schemes that are able to effectively damp high-frequency errors for all flow conditions.

In [1] we presented an optimization scheme to obtain optimal sequences of time-step values (i.e., a multi-stage scheme) for discretizations of the full Euler or Navier-Stokes spatial operator. Though this method was a step forward from earlier formulations, which based the design of the multi-stage schemes on either the scalar one-dimensional [2, 3] or two-dimensional [4] convection equation, the schemes obtained were not truly independent of flow conditions, such as Mach number and flow angle.

In [5] Allmaras pointed out that with semi-coarsening [6, 7], the high-frequency domain over which the multi-stage scheme must be a good damper of errors is reduced to "hi-hi" combinations (in 2-dimensions). This makes it easier to design optimal multi-stage schemes that are largely independent of flow conditions. In [8] we have obtained such multi-stage schemes and have shown that these multi-stage schemes, in conjunction with the semi-coarsened multigrid algorithm and local preconditioning [9], provide a fast and robust method for achieving steady-state Euler solutions.

In this paper we will present more detailed results, including solutions to model problems, to further substantiate this claim. Our research has also shown that Navier-Stokes operators require a different optimization formulation for the design of multi-stage schemes. This issue will also be addressed in this paper.

2 Semi-coarsening

When multi-dimensional convection is aligned with one of the grid directions, single-grid relaxation schemes cannot damp high-frequency errors propagating in the normal direction that are coupled to low frequency errors in the convection direction. This is known as the single-grid alignment problem.

Semi-coarsening is a method meant to resolve this grid-alignment problem in a multigrid context. Mulder [6, 7] has developed an efficient solver for the steady 2-D Euler equations based on semi-coarsening. The method employs semi-coarsening in two directions simultaneously (for a two-dimensional problem).

The usual restriction and prolongation operators have to be modified to handle input from more than one grid. If one grid needs data from two finer grids, the two sets of data obtained by the restriction from each finer grid are averaged. For prolongation, the correction is computed with respect to the latest fine-grid solution.

As pointed out earlier, with semi-coarsening, the high-frequency domain over which the multi-stage scheme must be a good damper of errors is reduced to "hi-hi" combinations, making it easier to design multi-stage schemes that are largely independent of flow conditions.

*Doctoral Candidate, Aerospace Engineering and Scientific Computing; Member AIAA

†Professor, Associate Fellow AIAA

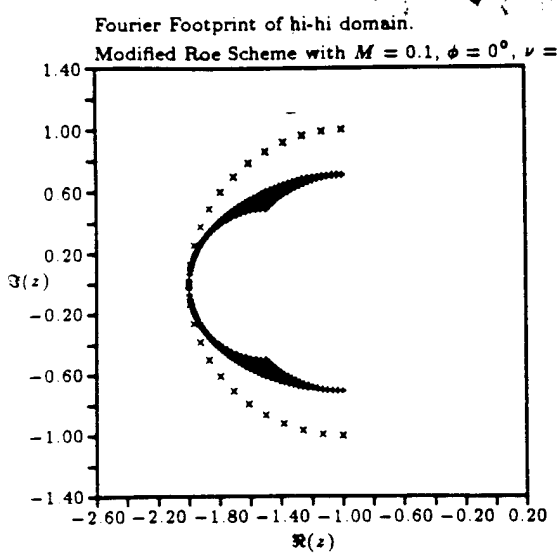

Figure 1: Fourier footprint of the first-order upwind approximation of the spatial Euler operator (modified Roe scheme) with the preconditioner of Van Leer et al. [9], for $M = 0.1$, and flow angle $\phi = 0°$. Footprint corresponds to hi-hi domain $|\beta_x|, |\beta_y| \in \left(\frac{\pi}{2}, \pi\right)$. The time-step chosen corresponds to a Courant-number value of 1.

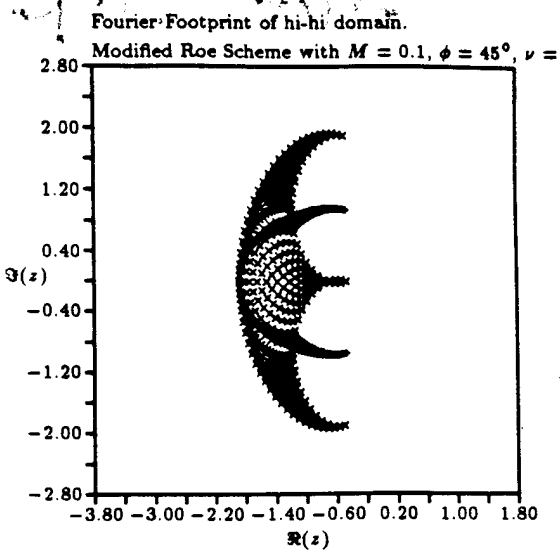

Figure 2: Fourier footprint of the $\kappa = 1/3$ upwind approximation of the spatial Euler operator with the preconditioner of Van Leer et al. [9], for $M = 0.1$, and flow angle $\phi = 45°$. Footprint corresponds to hi-hi domain $|\beta_x|, |\beta_y| \in \left(\frac{\pi}{2}, \pi\right)$. The time-step chosen corresponds to a Courant-number value of 1.

3 Local Preconditioning

Local preconditioning matrices attempt to remove the spread among characteristic speeds as much as possible. The matrix derived by Van Leer et al. [9] achieves what can be shown to be the optimal condition number for the characteristic speeds, namely, $1/\sqrt{1 - \min(M^2, M^{-2})}$, where M is the local Mach number. This is a major improvement over the condition number before preconditioning, which equals $(M + 1)/\min(M, |M - 1|)$.

The effect of local preconditioning on the discretizations of the spatial Euler operator is a strong concentration of the pattern of eigenvalues in the complex plane. This makes it possible to design multi-stage schemes that systematically damp most high-frequency waves admitted by a particular discrete operator [1]. The resulting schemes are not only preferable as solvers in a multi-grid strategy, they are also superior single-grid schemes, as the preconditioning itself already accelerates the convergence to a steady solution, and the high-frequency damping provides robustness.

The local preconditioning matrix described in [9] was derived based on the partial differential equations that make up the Euler equations. On analysis, it was realized that multigrid damping could be improved by modifying the matrix such that the high-frequency modes of all the waves overlap more completely. This modified Euler matrix is described in [10]. Figures 1 and 2 are presented as examples of the hi-hi frequency content in the Fourier footprints obtained with this modified preconditioner.

4 Optimization procedure for Euler Operators

The procedure for optimizing high-frequency damping aims at minimizing the maximum of the modulus of the scheme's amplification factor over a given set of high-frequency eigenvalues. The input parameters are the time-step values $\Delta t^{(k)}$, $k = 1, .., m$, of an m-stage algorithm. When updating the solution of

$$U_t = Res(U) \tag{1}$$

from time level t^n to $t^{n+1} = t^n + \Delta t$, the method takes the form

$$U^{(0)} = U^n, \tag{2}$$

$$U^{(k)} = U^{(0)} + \Delta t^{(k)} Res\left(U^{(k-1)}\right), \; k = 1, .., m, \tag{3}$$

$$U^{n+1} = U^{(m)} \tag{4}$$

with $\Delta t = \Delta t^{(m)}$. According to linear theory, one step with the full scheme multiplies each eigenvector of the operator $Res(U)$, with associated eigenvalue λ, by a factor of the form

$$P(z) = 1 + z + \sum_{k=2}^{m} c_k z^k, \tag{5}$$

where

$$z = \lambda \Delta t \tag{6}$$

generally is complex. The $m - 1$ coefficients c_k relate to the time-step *ratios* $\alpha_k = \Delta t^{(k)}/\Delta t$; the actual time step Δt is the mth parameter.

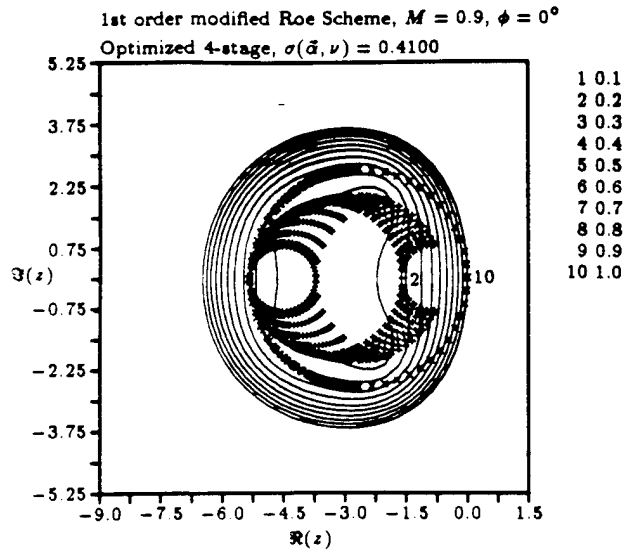

Figure 3: High-frequency Fourier footprint of the preconditioned first-order upwind Euler operator (modified Roe scheme with preconditioner of Van Leer et al. plotted on top of the level lines of the amplification factor of the associated optimal 4-stage scheme. Flow angle 0°, $M = 0.9$. Result of optimization over entire high-frequency domain minus wedge filter (cf. [1]).

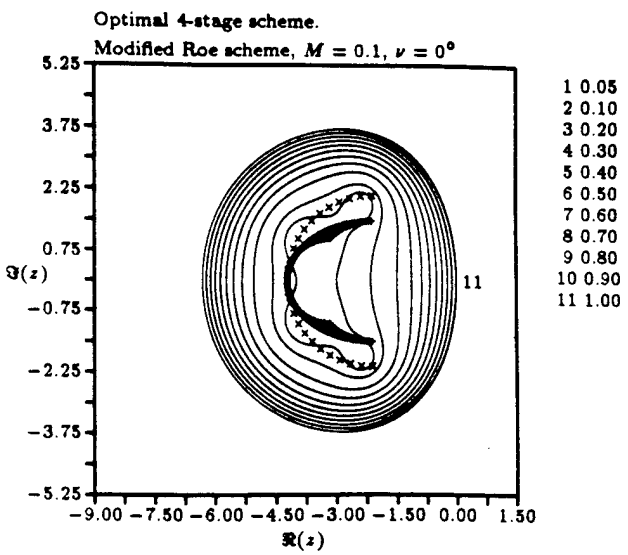

Figure 4: Optimal four-stage scheme obtained by optimizing over hi-hi frequency footprint of the modified Roe scheme with the preconditioner of Van Leer et al. [9]. $M = 0.1$, $\phi = 0$. $\sigma_{opt} = 0.0632$, $\nu = 2.108$.

Given a discrete Euler operator, the optimization procedure starts out by computing, for a fixed combination of M and ϕ ($\equiv$ flow angle), a discrete set of eigenvalues for wave-number pairs (β_x, β_y) in the high-frequency range, i.e.

$$|\beta_x| \in \left(\frac{\pi}{2}, \pi\right) \quad \text{and} \quad |\beta_y| \in \left(\frac{\pi}{2}, \pi\right). \tag{7}$$

Assuming a set of starting values for the m-stage scheme, for instance Tai's values [3], the value of $|P(z)|$ is computed for all eigenvalues previously obtained, and its maximum is found. This is our functional $\sigma(\Delta t^{(1)}, .., \Delta t^{(m)}; M, \phi)$; it must be minimized by varying the m parameters.

It is not a priori clear that the $\Delta t^{(k)}$ will be insensitive to values of M and ϕ. If, as in [1], we have to consider the whole high-frequency domain, i.e. $|\beta_x| \in \left(\frac{\pi}{2}, \pi\right)$ and/or $|\beta_y| \in \left(\frac{\pi}{2}, \pi\right)$, two problems arise: the alignment problem mentioned earlier and a singularity problem for $M \to 1$. Figure 3 gives evidence of both problems. There are lo-hi entropy/shear modes extending all the way into the origin, and hi-lo acoustic error modes at some distance to the origin that vanish as $\sqrt{1 - M^2}$. These two effects go away if we restrict ourselves to the high-frequency range (7) appropriate for semi-coarsening.

The optimal (in the L_∞ sense) m-stage scheme for a given discrete Euler operator may hence be obtained as the solution to the following minmax problem:

$$\sigma_{opt} = \min_{(\vec{\alpha}, \nu)} \left(\max_{|\beta_x|, |\beta_y| \in \left[\frac{\pi}{2}, \pi\right]} \|P(z(\beta_x, \beta_y, \nu), \vec{\alpha})\| \right). \tag{8}$$

This optimization problem is solved using the method of ***simulated annealing*** in conjunction with the ***downhill simplex*** algorithm of Nelder and Mead [11, 12].

Simulated annealing has proved to be both powerful and robust and the algorithm does not require frequent restarts (unlike Powell's method, which was used in [1]).

Figure 4 is an example of a scheme designed with the preconditioner of Van Leer et al.

4.1 Flow angle dependence

Any remaining flow-angle (ϕ) dependence may also be removed by appropriate definition of the Courant number ν. As in [1, 8], for the preconditioned Euler equations, with the characteristic speeds equal to or close to q, we define the Courant number as

$$\nu = q \frac{\Delta t}{l(\Delta x, \Delta y, \phi)}, \tag{9}$$

where l is a typical cell-width that may depend on the flow direction. For rectangular cells we find that defining

$$l = 1/(|\cos\phi| + \mathcal{AR}|\sin\phi|) \tag{10}$$

takes away most of the variation of ν with flow angle, so that a single value may be recommended. ([1] has this function defined incorrectly. The values of ν in the tables in this reference need to be scaled by a factor of $\sqrt{2}$ when using the above definition of l. [13] has updated tables).

Figure 5 shows the variation in Courant number with length scale independent of flow angle for a typical multi-stage scheme. As can be seen from the figure, our choice of length scale provides a fairly good fit to the variations. This allows us to recommend a single value of ν for each multi-stage scheme.

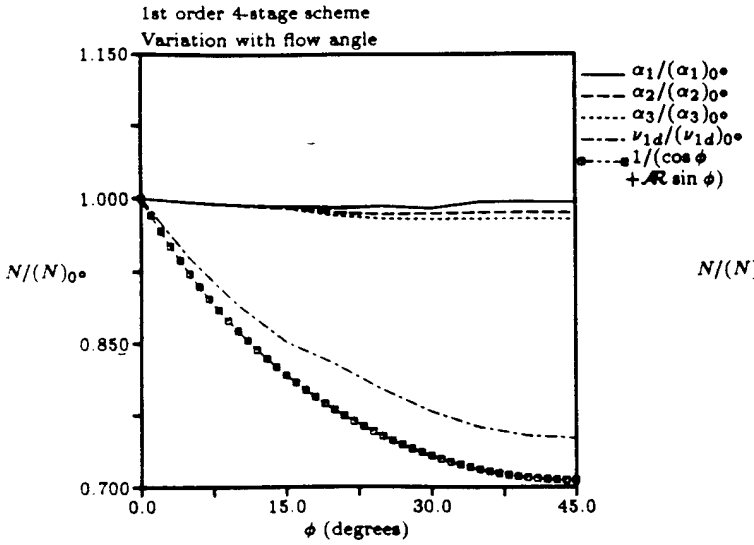

Figure 5: Variation with flow angle of multi-stage coefficients and Courant number (based on a fixed length scale independent of flow angle) for a first-order 4-stage optimal scheme. Optimization over hi-hi frequency domain only.

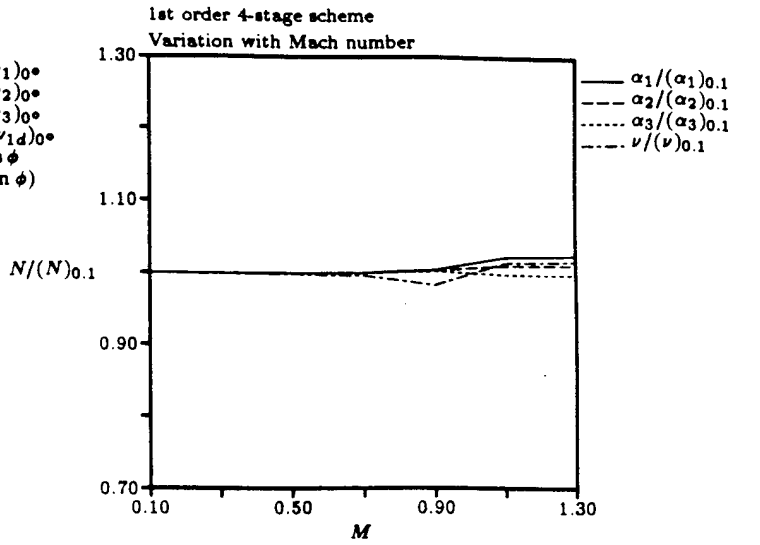

Figure 6: Variation of multi-stage coefficients and Courant number with Mach number for a first-order 4-stage optimal scheme. Optimization over hi-hi frequency domain only.

4.2 Dependence on Mach number

The Mach number dependence of the multi-stage schemes derived in the previous section was related to lo-hi acoustic error modes that had symbols at some distance to the origin that vanish as $\sqrt{1-M^2}$. The hi-hi frequency error-modes are fairly insensitive to Mach number, making it possible to design optimal multi-stage schemes with coefficients that are fairly insensitive to Mach number as well. Figure 6 shows the variation in the optimal multi-stage coefficients with Mach number. A slight change in the coefficients is observed while passing through the sonic point, but the change in values is small enough to allow us to recommend a single set of coefficients for each multistage scheme that may be applied over the entire Mach number and flow-angle range.

5 Optimization procedure for Navier-Stokes Operators

For Navier-Stokes preconditioners the idea put forth in [14] is to make the size of the footprint independent of cell-Reynolds number. This is achieved as follows. If we write the 2-D discretized Navier-Stokes equations as:

$$\mathbf{U}_t = L_{Eu}\mathbf{U} + (\mathbf{C}\mathbf{U}_x)_x + (\mathbf{D}\mathbf{U}_x)_y + (\mathbf{E}\mathbf{U}_y)_y, \qquad (11)$$

the first term on the right-hand side is the discrete Euler operator; the remaining terms are the viscous/conductive terms, assumed to be approximated by central differencing. These contribute only to the extent of the footprint along the negative real axis, which is inversely proportional to the cell-Reynolds number. The proper scaling required to make the size of the footprint independent of cell-Reynolds number is obtained by choosing $\mathbf{P}_{NS}$ as follows:

$$\mathbf{P}_{NS}^{-1} = \mathbf{P}_{Eu}^{-1} + \frac{2}{\Delta x}\mathbf{C} + \frac{2}{\Delta y}\mathbf{E}. \qquad (12)$$

For higher-order upwind differencing, the same scaling technique for the highest frequency Fourier footprints yields a similar expression:

$$\mathbf{P}_{NS}^{-1} = (1-\kappa)\mathbf{P}_{Eu}^{-1} + \frac{2}{\Delta x}\mathbf{C} + \frac{2}{\Delta y}\mathbf{E}. \qquad (13)$$

This strategy works for cell-Reynolds numbers that are not too low, e.g. $Re_{\Delta x} \geq 0.1$. For very low $Re_{\Delta x}$ a slight modification is needed in the continuity equation; this will be discussed elsewhere (cf. [15]).

With the above Navier-Stokes preconditioning, we are able to design a family of multi-stage schemes that are dependent only on cell-Reynolds number. We would hope that as the cell-Reynolds number decreases, the time steps required for good damping increase, as the high-frequency content in the footprint begins to align itself along the negative real axis. This, unfortunately, does not happen if we make use of the above optimization procedure for a discrete, preconditioned Navier-Stokes operator with prescribed values of Mach number, flow angle and cell-Reynolds number. The formulation described above attempts to maximize the damping over the domain, which results in extremely (unnecessarily) small functional (σ_{opt}) values for the corresponding multi-stage schemes. The stronger damping comes at a price - smaller Courant numbers for these time-stepping schemes. This means taking smaller time-steps, thereby increasing the number of computational steps required to attain a converged solution. Since the cell length-scales used in computing these time-steps tend to be small (a common feature of high-Reynolds number computations), the larger the Courant number of

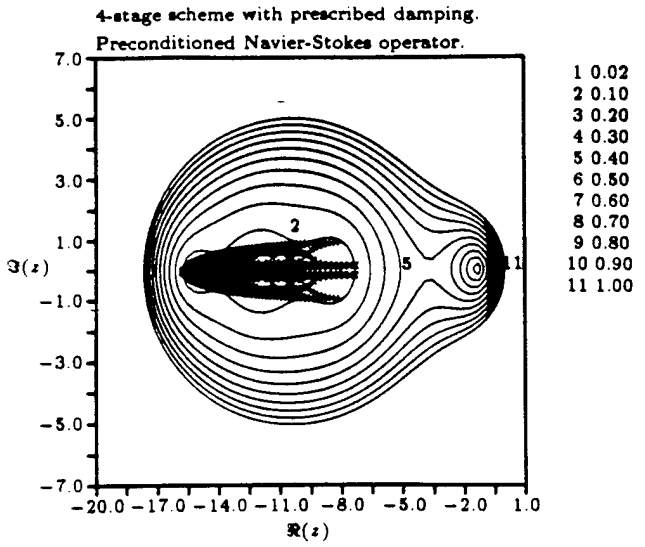

Figure 7: Four-stage scheme obtained by optimizing over hi-hi frequency footprint of the discrete, preconditioned Navier-Stokes operator. σ_{min} was prescribed as 0.1. $M = 0.1$, $\phi = 0$, $Re_{\Delta x} = 0.1$, $\mathcal{AR} = 1$. $\nu = 7.891$.

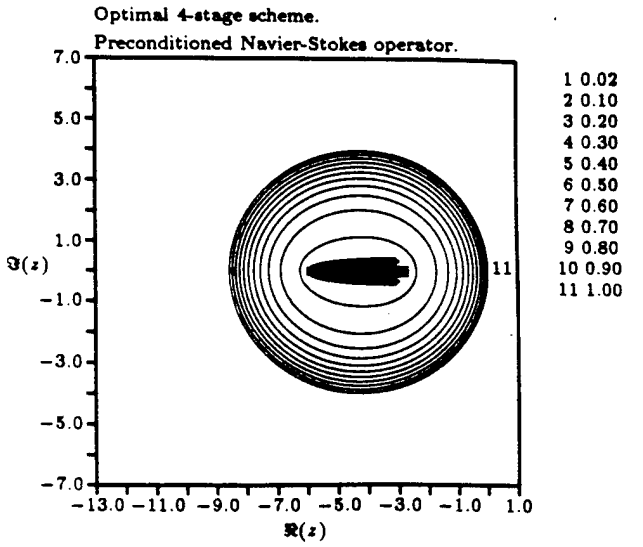

Figure 8: Optimal four-stage scheme obtained by optimizing over hi-hi frequency footprint of the discrete, preconditioned Navier-Stokes operator. $M = 0.1$, $\phi = 0$, $Re_{\Delta x} = 0.1$, $\mathcal{AR} = 1$. $\sigma_{opt} = 0.0034$, $\nu = 2.953$.

the scheme, the better. It is therefore obvious that a different approach is necessary for Navier-Stokes operators.

For Navier-Stokes operators, we have redefined the optimization problem as follows: *For a given spatial operator, find the largest Courant number with which the corresponding multi-stage scheme has a prescribed damping capability.*

This may be written as:

$$\text{Solve} \quad \sigma(\nu) = \sigma_{min} \tag{14}$$

where $\sigma(\nu)$ is defined below:

$$\sigma(\nu) = \min_{\vec{\alpha}} \left(\max_{|\beta_x|,|\beta_y| \in \left[\frac{\pi}{2},\pi\right]} \|P(z(\beta_x,\beta_y,\nu),\vec{\alpha})\| \right).$$

The solution to this problem is fairly simple. We make the assumption that $\sigma(\nu)$ is a continuous, monotonically-increasing function within our range of interest. (This seems to be a valid assumption from our experiments). We may then search for a root to equation (14) using an algorithm such as the *bisection* method (cf. [11]) or the more complex algorithm due to Brent [12] which combines the sureness of the bisection method with the speed of a higher order method when appropriate. Each evaluation of $\sigma(\nu)$ requires a solution to the underlying optimization problem (which may be solved using simulated annealing as before). Care must therefore be taken to ensure that an appropriate set of starting values of $\vec{\alpha}$ are used for each evaluation of $\sigma(\nu)$. Another point of concern is the choice of σ_{min}. Too large a value of σ_{min} can result in a scheme that is unstable for frequency modes other than the "hi-hi" combinations being considered. Figure 9 is an example of such a scheme.

Figure 7 is an example of a scheme designed using this procedure. In contrast, Figure 8 shows a scheme designed using the optimization procedure described earlier. As can be seen from the figures, the two schemes have different damping properties. By prescribing the damping factor σ_{min} to be 0.1, the new scheme's Courant number increases to 7.89 from 2.95 with the earlier formulation.

This approach is not well suited for discretizations of the Euler operator. The increase in Courant number is marginal at best. Navier-Stokes footprints tend to align themselves along the real axis in the complex plane with decreasing cell-Reynolds number (as the behavior becomes increasingly parabolic). Increasing the Courant number causes the footprint to grow primarily in this direction for these operators. Euler footprints grow outward in all directions at the same rate, making it more difficult to obtain time-stepping schemes that damp all error-modes.

One way of avoiding multi-stage coefficients that amplify some error-modes, as in Figure 9, is by adding in a constraint to the formulation. An appropriate constraint would be

$$P_{max} \equiv \max_{|\beta_x|,|\beta_y| \in [0,\pi]} \|P(z(\beta_x,\beta_y,\nu),\vec{\alpha})\| \leq 1. \tag{15}$$

This constrained-optimization problem (equations (14) and (15)) can be reformulated as an unconstrained-optimization problem by making use of a penalty function. We can write $\sigma(\nu)$ as

$$\begin{aligned} \sigma(\nu) \quad = \quad & \min_{\vec{\alpha}} \Big(\max_{|\beta_x|,|\beta_y| \in \left[\frac{\pi}{2},\pi\right]} \|P(z(\beta_x,\beta_y,\nu),\vec{\alpha})\| \\ & + \gamma(P_{max} - 1)^2 \Big), \end{aligned} \tag{16}$$

where γ is a constant, $\gamma \geq 0$. The larger γ is, the more

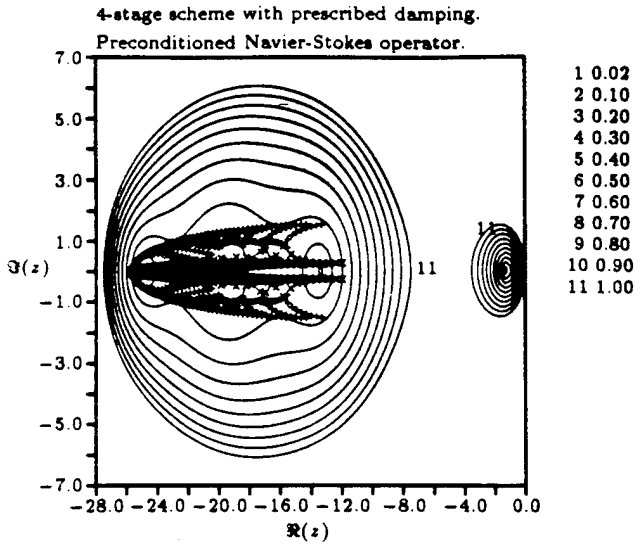

Figure 9: Four-stage scheme obtained by optimizing over hi-hi frequency footprint of the discrete, preconditioned Navier-Stokes operator. σ_{min} was prescribed as 0.2. $M = 0.1$, $\phi = 0$, $Re_{\Delta x} = 0.1$, $\mathcal{AR} = 1$. $\nu = 12.845$. It is obvious that this scheme will be unstable for some "hi-lo", "lo-hi" and "lo-lo" frequency combinations.

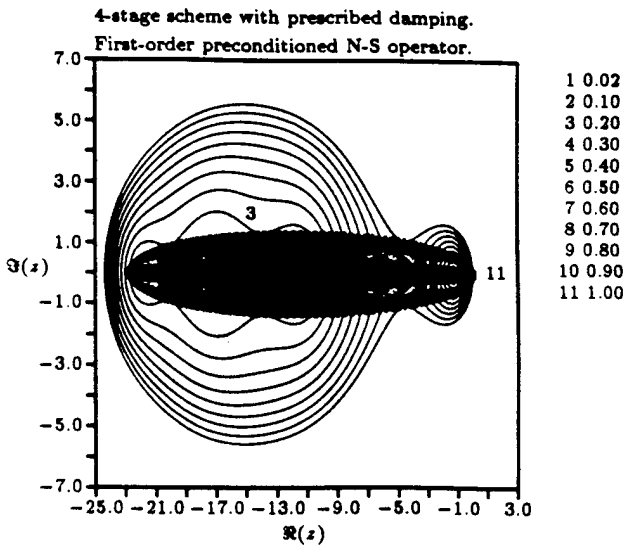

Figure 10: Four-stage scheme obtained by optimizing over hi-hi frequency footprint of the discrete, preconditioned Navier-Stokes operator with a constraint on P_{max} introduced via a penalty function. The entire footprint is shown here. σ_{min} was prescribed as 0.2. $M = 0.1$, $\phi = 0$, $Re_{\Delta x} = 0.1$, $\mathcal{AR} = 1$. $\nu = 11.3679$.

strongly is the constraint enforced. Taking too large a value of γ however can affect the robustness of the optimization algorithm. We found that taking taking a modest value of γ initially (around 100) and then recomputing the solution with this trial solution and γ around 1×10^6 worked well in enforcing the constraint. Figure 10 is an example of a solution obtained in this manner. We have obtained a stable scheme with only a modest decrease in Courant number. It is unclear however if this scheme will perform well in nonlinear implementations. Certain modes are likely to be excited if the time-step taken corresponds to even a modest increase over the prescribed value. One option is to modify our constraint to allow for some variation in the Courant number without encountering amplification factors greater than one for some wave-modes. This modified constraint could be written as

$$P^{\delta}_{max}(\nu) \equiv \max_{\eta=\nu,\nu(1+\delta)} \left(\max_{|\beta_x|,|\beta_y| \in [0,\pi]} \|P(z,\vec{\alpha})\| \right) \leq 1, \quad (17)$$

where $z = z(\beta_x, \beta_y, \nu)$. The optimization problem may be formulated as an unconstrained optimization problem as before. Figure 11 is an example of the solution to this problem with $\delta = 0.2$. These coefficients are likely to be more reliable in a multigrid formulation than the coefficients derived earlier.

Choosing a lower value for σ_{min}, say around 0.12, for the case considered in Figure 11, would obviate the need for the constraint (eqn. 17) and its associated complications.

It is unclear what is the best choice for σ_{min} in terms of obtaining the best possible multigrid convergence rates. This could likely be determined from multigrid studies involving preconditioned Navier-Stokes operators and various test conditions. Multi-stage schemes with $\sigma = 0.2$ and more have worked well in our multigrid Euler studies (though we did not attempt to prescribe the magnitude of damping here). Similar multigrid studies remain to be undertaken with the preconditioned Navier-Stokes equations.

5.1 Multi-stage coefficients with prescribed damping for Navier-Stokes operators

When following this approach, it is unlikely that we would be able to recommend a single set of coefficients independent of $Re_{\Delta x}$ and $\mathcal{AR}$. A likely compromise would be to generate curve-fits to account for the variations in coefficients due to each of these parameters.

As a preliminary study we have obtained the coefficients for a four-stage time stepping scheme based on the Fourier footprint of the discrete, preconditioned first-order Navier-Stokes operator, discretized using the modified Roe scheme for inviscid terms and central differencing for the viscous terms. The variation in the coefficients with cell-Reynolds number was studied. Figure 12 shows these variations, normalized to the values of the coefficients for the Euler operator. The figure indicates that the optimal Courant number increases sharply as the cell-Reynolds number decreases, while the multi-stage coefficients decrease. It would seem that curve-fits in terms of $\log(Re_{\Delta x})$ are feasible.

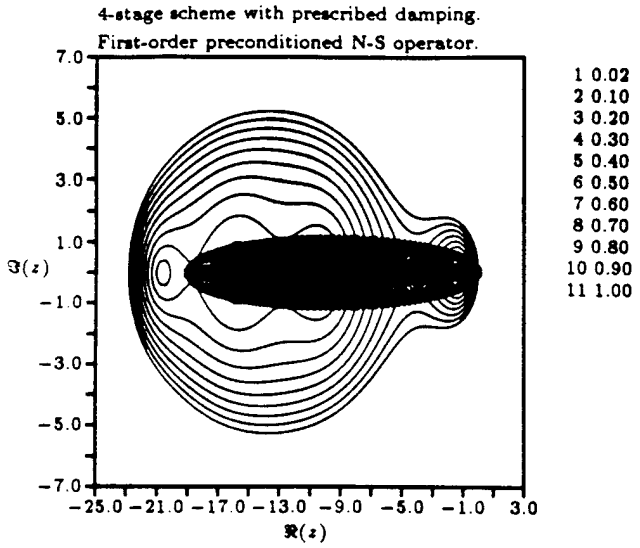

Figure 11: Four-stage scheme obtained by optimizing over hi-hi frequency footprint of the discrete, preconditioned Navier-Stokes operator with a constraint on P^{δ}_{max} (eqn. 17) introduced via a penalty function. The entire footprint is shown here. σ_{min} was prescribed as 0.2. $M = 0.1$, $\phi = 0$, $Re_{\Delta x} = 0.1$, $\mathcal{AR} = 1$. $\delta = 0.2$. $\nu = 9.5361$.

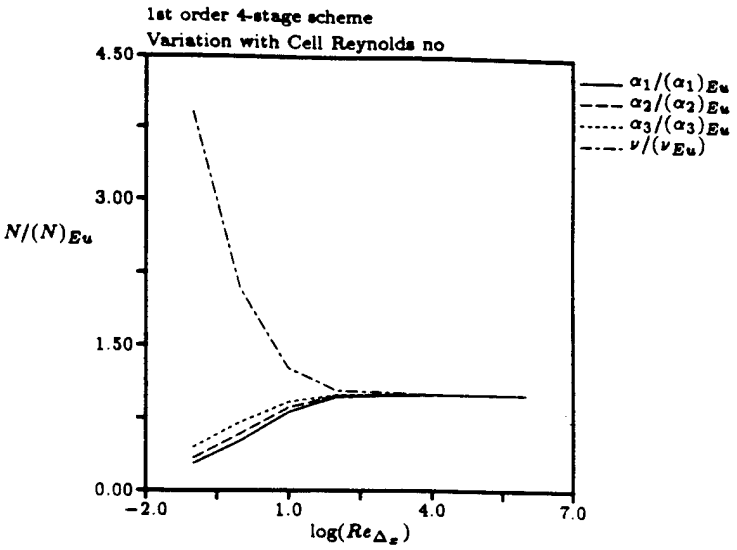

Figure 12: Variation with cell-Reynolds number of multistage coefficients and Courant numver for a first order 4-stage scheme with prescribed damping. Optimization based hi-hi frequency footprint of the discrete, preconditioned Navier-Stokes operator with a constraint on P_{max} introduced via a penalty function. σ_{min} was prescribed as 0.15. $M = 0.1$, $\phi = 0$, $\mathcal{AR} = 1$, $\delta = 0.05$.

5.2 Optimal multi-stage schemes for the preconditioned Euler equations

We have computed optimal multi-stage schemes based on the modified Roe discrete operator for the preconditioned Euler equations with the preconditioner of Van Leer et al. These coefficients are presented as tables in [13, 8], and have been used to obtain the results in this paper. For completeness, a condensed version of these tables is presented here; see Tables 1-4.

These schemes are not only preferable as solvers in a multigrid strategy, but are also superior single-grid schemes, as the preconditioning itself already accelerates the convergence to a steady solution and the high-frequency damping provides robustness.

6 Multigrid Euler Solutions

The preconditioner of Van Leer et al. has been shown to produce dramatic speed-ups for steady solutions to the problem of "flow past a semi-circular bump ($t/c = 0.042$) in a channel" [8]. The modified Roe scheme that is used here also provides more accurate solutions for cases with low freestream Mach number. Results of these runs are shown in Tables 5 and 6 in terms of equivalent work units. A work unit is the amount of work required to compute a single-stage update on the fine grid. These are the "best" single and multigrid results obtained from multiple runs using 2-6 (3-6 for second order) stages and 1-5 (1-4 for second order) grid levels. The second-order solutions made use of Van Albada's limiter and defect-correction multigrid cycles for the multigrid cases. Figures 14, 15 and 16 are examples of solutions obtained with this method.

Tables 5 and 6 indicate that local and matrix time-stepping require similar amounts of work in the single-grid subsonic and transonic runs. This is probably an artifact of the problem. (This behavior is not observed when solving for the flow in a semi-infinite channel). The reflective wall-boundary conditions in the channel provide minimal attenuation of acoustic error-modes and this effect dominates single-grid convergence. This is not a problem for the supersonic cases, which have a largely convective nature. The speed-up of multigrid with local preconditioning over multigrid with local time-stepping is a lot more dramatic; the former is 3-4 times faster in all cases. Convergence in the subsonic and transonic cases is also an order of magnitude faster than in the corresponding single-grid cases. Local preconditioning performs admirably on a single-grid for the supersonic case, and there is not much improvement possible without modifying multigrid to better handle convection-dominated flow.

A semi-coarsened multigrid cycle is more expensive than a regular multigrid cycle (a factor of three on average for the cases considered - this factor depends on the number of grid levels and number of stages chosen). Each semi-coarsened multigrid cycle is able to reduce the residual norm by a larger factor than a corresponding regular multigrid cycle. However, some of the extra overhead that is inherent in the method does show up in the work required to obtain the same solution with the same number of grid levels and stages in the time-stepping scheme. Tables 5 and 7 refect the difference in work required. It should be pointed out though that the semi-coarsened

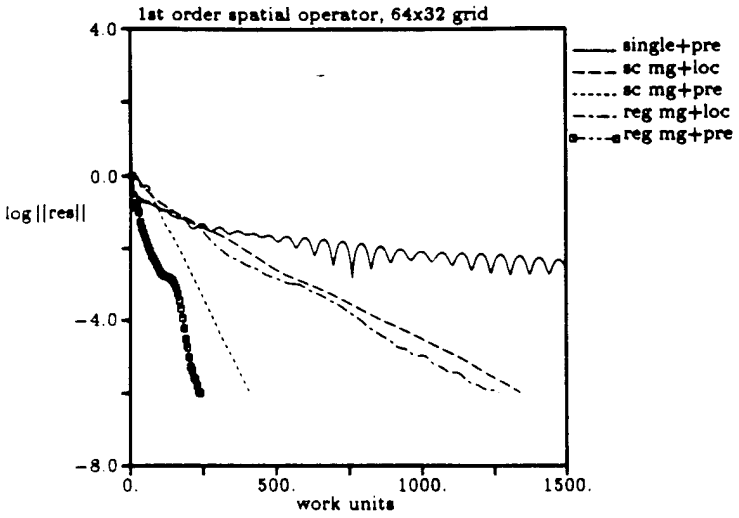

Figure 13: Residual history plots for the transonic test case considered above ($M = 0.85$). 64x32 grid. All runs were made with four-stage time-stepping schemes and all multigrid runs made with four levels (8x4 as coarsest grid).

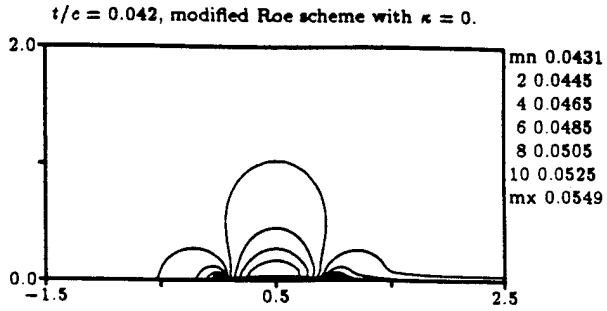

Figure 14: Mach number contours. Subsonic flow past a bump in a channel. Modified Roe scheme with the preconditioner of Van Leer et al. $\kappa = 0$ variable extrapolation. 128x64 grid. Solution obtained with semi-coarsened multigrid incorporating an optimal four-stage scheme. $M = 0.05$, $t/c = 0.042$.

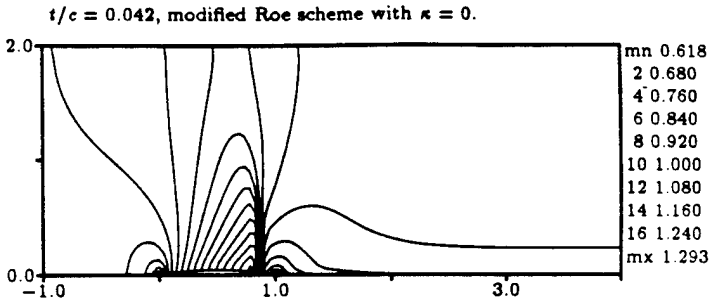

Figure 15: Mach number contours. Transonic flow past a bump in a channel. Modified Roe scheme with the preconditioner of Van Leer et al. $\kappa = 0$ variable extrapolation with Van Albada's limiter. 128x64 grid. Solution obtained with semi-coarsened multigrid incorporating an optimal four-stage scheme. $M = 0.85$, $t/c = 0.042$.

multigrid method makes up for the extra work required in the form of increased robustness. Residual history plots indicate that the convergence rate with regular multigrid can be erratic, especially in the transonic regime, whereas it is essentially constant with semi-coarsening (see Figure 13). Also, in our calculations, regular multigrid exhibited extremely poor convergence rates (especially with local-timestepping) when attempting to obtain a second-order spatially accurate solution to the transonic case ($M = 0.85$).

6.1 Improving robustness

The preconditioner of Van Leer et al. is known to be lacking in robustness about sonic and stagnation points. The stagnation-point singularity appears to be quite a difficult problem to correct and there has been substantial research in this area (cf. [16, 17]).

The sonic-point singularity may be overcome more easily. The scaling parameter $\beta = \sqrt{|1 - M^2|}$ is present in the denominator of some terms in the preconditioner of Van Leer et al. as well as in the denominator of certain terms in the modified Roe flux function. These become unbounded as $M \to 1$, at which point $\beta \to 0$.

One obvious fix is to bound β away from zero by some artificial means, such as a smoothing function.

We opted to fit a parabolic curve to β such that the fit matched the curve $\sqrt{1 - M^2}$ for a given value of M in both value and slope. The point of intersection with the other branch, $\sqrt{M^2 - 1}$, was also required to match in slope. Since only three conditions can be specified for this curve-fit, we opted not to specify the point of intersection with the curve $\sqrt{M^2 - 1}$ (cf. [13]).

With this approach and in conjunction with explicit

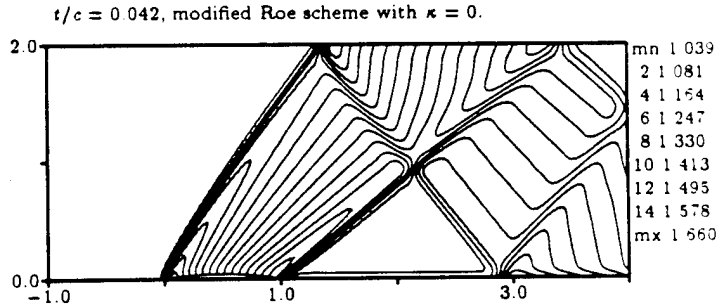

Figure 16: Mach number contours. Supersonic flow past a bump in a channel. Modified Roe scheme with the preconditioner of Van Leer et al. $\kappa = 0$ variable extrapolation with Van Albada's limiter. 128x64 grid. Solution obtained with semi-coarsened multigrid incorporating an optimal four-stage scheme. $M = 1.4$, $t/c = 0.042$.

Number of Stages

	2	3	4	5	6
α_1	0.3333	0.1467	0.08125	0.05204	0.03712
α_2	1	0.3979	0.2033	0.1240	0.08516
α_3		1	0.4226	0.2343	0.1521
α_4			1	0.4381	0.2566
α_5				1	0.4525
α_6					1
ν	1.0000	1.5252	2.1058	2.6824	3.0827
σ_{opt}	0.3333	0.1418	0.06328	0.03024	0.01627

Table 1: Optimal multi-stage coefficients for first-order scheme. Optimization based on hi-hi high frequency domain.

Number of Stages

	2	3	4	5	6
α_1	0.5713	0.2239	0.1299	0.08699	0.06134
α_2	1	0.5653	0.2940	0.1892	0.1322
α_3		1	0.5604	0.3263	0.2201
α_4			1	0.5558	0.3425
α_5				1	0.5531
α_6					1
ν	0.6305	1.0458	1.4008	1.7471	2.0701
σ_{opt}	0.6475	0.4279	0.2927	0.2047	0.1464

Table 2: Optimal multi-stage coefficients for $\kappa = 0$ scheme. Optimization based on hi-hi high frequency domain.

Number of Stages

	2	3	4	5	6
α_1	0.4450	0.1780	0.09900	0.06431	0.04540
α_2	1	0.4774	0.2434	0.1509	0.1044
α_3		1	0.4913	0.2783	0.1846
α_4			1	0.5004	0.3030
α_5				1	0.5116
α_6					1
ν	0.4386	0.7439	1.0139	1.2608	1.4613
σ_{opt}	0.6154	0.3916	0.2526	0.1654	0.1145

Table 3: Optimal multi-stage coefficients for $\kappa = -1$ scheme. Optimization based on hi-hi high frequency domain.

Number of Stages

	2	3	4	5	6
α_1	0.6826	0.2695	0.1572	0.1085	0.07727
α_2	1	0.6351	0.3350	0.2180	0.1537
α_3		1	0.6079	0.3581	0.2428
α_4			1	0.5887	0.3650
α_5				1	0.5729
α_6					1
ν	0.7167	1.1704	1.5694	1.9924	2.4407
σ_{opt}	0.6677	0.4454	0.3171	0.2336	0.1686

Table 4: Optimal multi-stage coefficients for $\kappa = 1/3$ scheme. Optimization based on hi-hi high frequency domain.

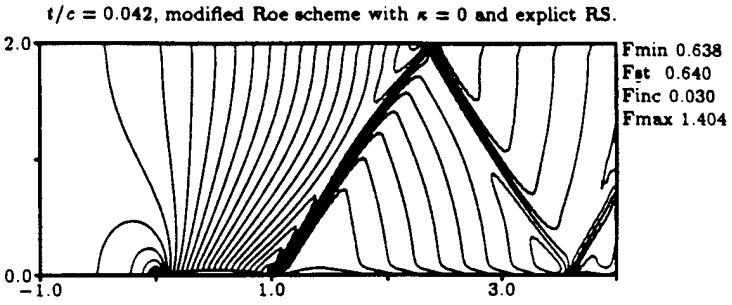

Figure 17: Mach number contours. Flow past a non-smooth bump in a channel. $M = 1.0$, $t/c = 0.042$, 128×64 grid. $\kappa = 0$ variable extrapolation with modified Roe scheme and Van Albada's limiter. Explicit residual-smoothing was used to obtain this solution.

residual smoothing, we were able to obtain a solution to the channel problem with a freestream Mach number $M = 1$. Figure 17 shows this solution.

7 Multigrid for Navier-Stokes Operators

Just as for Euler discretizations, the multi-stage schemes described above for discrete Navier-Stokes operators should be an ideal choice as the basic relaxation scheme in a semi-coarsened multigrid strategy. Multigrid applications of the optimized multi-stage schemes will be presented in [15].

8 Conclusions

We have demonstrated that the combination of local preconditioning and multi-stage time-stepping can produce relaxation schemes that boast guaranteed, strong

	$M = 0.35$		$M = 0.85$		$M = 1.4$	
	Local TS	Matrix TS	Local TS	Matrix TS	Local TS	Matrix TS
Single	2940	2520	4140	4920	1550	355
Multigrid	1123	268	911	326	651	234

Table 5: Comparison of first-order convergence rates for flow past a semi-circular bump in a channel, 64x32 grid. Work units required to reduce the norm of the residual by five orders of magnitude. (Local TS ≡ local time-stepping, Matrix TS ≡ local preconditioning). Semi-coarsened multigrid.

	$M = 0.35$		$M = 0.85$		$M = 1.4$	
	Local TS	Matrix TS	Local TS	Matrix TS	Local TS	Matrix TS
Single	3685	2380	5305	9600	1344	414
Multigrid	582	191	515	167	722	309

Table 6: Comparison of second-order ($\kappa = 0$) convergence rates for flow past a semi-circular bump in a channel, 64x32 grid. Work units required to reduce $\|TE\|_1$ (cf. [7]) to 10^{-2} for $M = 0.35$ and $M = 1.4$ and to 5×10^{-2} for $M = 0.85$. Nested iteration with 5 defect-correction sweeps on each coarse grid level was used initially to improve robustness for multigrid solutions. Semi-coarsened multigrid.

	$M = 0.35$		$M = 0.85$		$M = 1.4$	
	Local TS	Matrix TS	Local TS	Matrix TS	Local TS	Matrix TS
Single	2940	2130	4140	4150	1550	288
Multigrid	892	165	752	174	514	161

Table 7: Comparison of first-order convergence rates for flow past a semi-circular bump in a channel, 64x32 grid. Work units required to reduce the norm of the residual by five orders of magnitude. Regular multigrid.

high frequency damping for the entire range of flow angles, Mach numbers and cell-Reynolds numbers. Such schemes are ideally suited for use as single-grid relaxation schemes in a multigrid relaxation framework, particularly if semi-coarsening is used.

Some numerical results are presented to support this claim; more multigrid experimenting is needed to determine the best balance between parameters such as damping rate and time-step value.

Acknowledgements

The research reported here was carried out under AFOSR grant number F49620-92-J-0158-DEF.

References

[1] J. F. Lynn and B. van Leer, "Multi-stage schemes for the Euler and Navier-Stokes equations with optimal smoothing," in *AIAA 11th Computational Fluid Dynamics Conference*, 1993.

[2] A. Jameson, "Numerical solution of the Euler equations for compressible inviscid fluids," in *Numerical Methods for the Euler Equations of Fluid Dynamics* (F. Angrand, A. Dervieux, J. A. Désidéri, and R. Glowinski, eds.), SIAM, 1985.

[3] B. van Leer, C. H. Tai, and K. G. Powell, "Design of optimally-smoothing multi-stage schemes for the Euler equations," in *AIAA 9th Computational Fluid Dynamics Conference*, 1989.

[4] L. A. Catalano and H. Deconinck, "Two-dimensional optimization of smoothing properties of multi-stage schemes applied to hyperbolic equations," in *Proceedings of the Third European Conference on Multigrid Methods*, 1990.

[5] S. Allmaras, "Analysis of a local matrix preconditioner for the 2-D Navier-Stokes equations," in *AIAA 11th Computational Fluid Dynamics Conference*, 1993.

[6] W. Mulder, "A new multigrid approach to convection problems," *Journal of Computational Physics*, vol. 83, 1989.

[7] W. Mulder, "A high-resolution Euler solver based on multigrid, semi-coarsening and defect correction," *Journal of Computational Physics*, vol. 100, 1991.

[8] J. F. Lynn and B. van Leer, "Multigrid Euler solutions with semi-coarsening and local preconditioning," in *14th International Conference on Numerical Methods in Fluid Dynamics*, 1994.

[9] B. van Leer, W. T. Lee, and P. L. Roe, "Characteristic time-stepping or local preconditioning of the Euler equations," in *AIAA 10th Computational Fluid Dynamics Conference*, 1991.

[10] D. Lee and B. van Leer, "Progress in local preconditioning of the Euler and Navier-Stokes equations," in *AIAA 11th Computational Fluid Dynamics Conference*, 1993.

[11] W. Press, S. Teukolsky, W. Vetterling, and B. Flannery, *Numerical Recipes. The Art of Scientific Computing. Second Edition.* Cambridge University Press, 1992.

[12] R. P. Brent, *Algorithms for Minimization without Derivatives.* Prentice-Hall, Englewood Cliffs, N.J., 1973.

[13] J. F. Lynn, *Multigrid solution of the Euler equations with local preconditioning.* PhD thesis, University of Michigan, 1995.

[14] A. G. Godfrey, R. W. Walters, and B. van Leer, "Preconditioning for the Navier-Stokes equations with finite-rate chemistry," AIAA Paper 93-0535, 1993.

[15] D. Lee, *Local Preconditioning of the Euler and Navier-Stokes equations (in preparation).* PhD thesis, University of Michigan, 1995.

[16] B. van Leer, E. Turkel, C.-H. Tai, and L. Mesaros, "Preconditioning in a stagnation point," in *AIAA 12th Computational Fluid Dynamics Conference*, 1995.

[17] D. L. Darmofal and P. J. Schmid, "The importance of eigenvectors for local preconditioners of the Euler equations," in *AIAA 12th Computational Fluid Dynamics Conference*, 1995.